

## Article

# Hot Days and Heat Waves in Poland in the Period 1951–2019 and the Circulation Factors Favoring the Most Extreme of Them

Joanna Wibig 

Department of Meteorology and Climatology, University of Lodz, 90-139 Lodz, Poland;  
joanna.wibig@geo.uni.lodz.pl

**Abstract:** The aim of the study is to analyze the occurrence of hot days and heat waves in Poland, their intra-annual distribution, and their long-term variability, and to present the circulation factors favoring the appearance of extensive waves in the country. Hot days were days with  $T_{max}$  not lower than the threshold value defined by the 95th percentile of summer  $T_{max}$  in the period 1961–1990. Atmospheric circulation was described using sea level pressure, geopotential of 700 and 500 hPa level, and horizontal and vertical wind on these levels. A statistically significant increase in the number of hot days in the entire study period and a significant acceleration in growth after 1980 were shown. In the entire analyzed period, only 11 waves were found covering at least 25% of the country area and lasting no less than a week. Among them, only one occurred before 1990, and more than half were observed in the last decade. Four circulation patterns favoring the extensive heat waves were distinguished differing the location of main baric center location. Spatial and temporal distribution of vertical velocity anomalies allows distinguishing clear phases of strengthening, stabilization, and weakening of anticyclone accompanying the occurrence of a heat wave.

**Keywords:** temperature extremes; spatial extent; long-term variability; atmospheric circulation; subsidence



**Citation:** Wibig, J. Hot Days and Heat Waves in Poland in the Period 1951–2019 and the Circulation Factors Favoring the Most Extreme of Them. *Atmosphere* **2021**, *12*, 340. <https://doi.org/10.3390/atmos12030340>

Academic Editor: Arkadiusz Marek Tomczyk

Received: 8 February 2021  
Accepted: 3 March 2021  
Published: 6 March 2021

**Publisher's Note:** MDPI stays neutral with regard to jurisdictional claims in published maps and institutional affiliations.



**Copyright:** © 2021 by the author. Licensee MDPI, Basel, Switzerland. This article is an open access article distributed under the terms and conditions of the Creative Commons Attribution (CC BY) license (<https://creativecommons.org/licenses/by/4.0/>).

## 1. Introduction

Contemporary climate change is manifested by evidence of an intense increase in surface temperature of the Earth [1]. In recent years, the temperature rise has accelerated. According to World Meteorological Organization (WMO) [2], the past five years, 2015–2019, were the five warmest on record. The observed warming is accompanied by an increase in frequency and intensity of extreme air temperature values, including heat waves. In developed countries, heat waves are regarded as a major cause of weather-related fatalities [3–6].

After 1990, there have been several heat waves covering extensive areas of Europe. In Poland and Czech Republic, the heat wave which occurred in 1994 was very intensive and widespread [7–9]. A lot of attention has been devoted to the 2003 heat wave over Central European countries [10–12], followed by another exceptional heat wave in July of 2006 in Central Europe [9], the heat wave in July 2010 in Eastern Europe [13–16], and the heat wave in Central Europe in August 2015 [17,18]. Due to global warming, it is very likely that the frequency and intensity of such events will increase in the future [19,20].

Heat waves in Poland have been analyzed by several authors. Wibig [8] has shown that the frequencies of very warm and hot days increased in the period 1951–2006, especially in the second part of this period (1979–2006). Heat waves were also analyzed at selected sites in the Wyżyna Kielecka [21] and in Warsaw [22]. Twardosz and Kossowska-Cezak [23] analyzed thermal extremes in Central Europe on the basis of data from 54 stations. They distinguished extremely hot summers, that is, summers having an average temperature equal to or greater than the long-term average plus two standard deviations, and analyzed the frequencies of days with  $t_{max}$  exceeding selected thresholds. Krzyżewska

and Wereski [24] analyzed waves of both heat and cold in bioclimatic regions over the short period of 2000–2010.

In numerous European studies, the occurrence of heat waves has been associated with several factors. Some authors pointed to the presence of high-pressure systems blocking the zonal circulation as a cause of heat waves [17,25–27]. Some papers indicate that the blocking patterns should be accompanied by low-pressure systems south of 55° N [28–30]. Others underline the role of persistent anticyclones in generating subsidence [11,15,31]. Participation of the anticyclones associated with quasi-stationary Rossby waves over mid-high latitudes in Europe and Eurasia in the prolonged heat waves was demonstrated [32,33]. Apart from the atmospheric pressure anomalies, land–atmosphere interactions are often suggested as a cause of heat wave generation [34,35]. Ref. [34] pointed out deficiency of soil moisture as a possible factor of heat wave generation. Positive feedback between deficiency of soil moisture and enhanced air temperature was also described [35].

The objective of the study was the description of the occurrence of heat waves in Poland in the period 1951–2019 with a particular emphasis on those that occurred simultaneously for a long time on the large area of the country. The other goal was to show the influence of atmospheric circulation on their formation, intensity, and persistence. In addition, the aim was to analyze the vertical velocity as a factor of heat wave development.

The second section presents the data and the methods used. The third section presents in turn: heat wave statistics and their long-term variability, types of atmospheric circulation during which extensive and long-lasting heat waves occur, and the variability of vertical velocity during various phases of heat wave development. Discussion is presented in section four and conclusions in section five.

## 2. Materials and Methods

Heat waves in Poland are described using maximum daily temperature records from 40 meteorological stations in Poland covering the period 1951–2019. The locations of these stations are presented in Figure 1. Data were obtained from the archive datasets of the Institute of Meteorology and Water Management—National Research Institute (IMWM-NRI) in Poland. The data published by IMWM-NRI are quality controlled. Breaks in measurements were supplemented using data from a few neighboring stations. At any of the selected stations, gaps did not exceed 1%. At one station (Rzeszów), the data starts from January 1952, and at another (Lesko), from June 1954. They both are located in the southeast of the country.



Figure 1. Locations of stations with Tmax data.

To describe the atmospheric circulation, the sea level pressure (SLP), geopotential heights (HGT), horizontal wind, and vertical velocity in pressure coordinates of 700 and 500 hPa levels from the database of the National Centre for Environmental Prediction/National Centre for Atmospheric Research (NCEP/NCAR) (<https://psl.noaa.gov/data/gridded/data.ncep.reanalysis.html>, accessed on 1 December 2020) [36] were obtained. Data from the area 60° W to 60° E and 30–70° N were extracted for this paper. The data are in 2.5° × 2.5° resolution, and a total of 833 grid-cells were used. Monthly values from the period 1951–2019 were used for calculating long-term average monthly values. Daily values from selected days were used to analyze conditions during heat waves.

The literature provides three groups of definitions based on relative and absolute thresholds. The first group uses absolute thresholds and a heat wave is defined as a sequence of at least three days with maximum daily temperature equal to or higher than 30 °C [8,25,37,38]. The second group of definitions is based on the thresholds defined using the statistical distribution of Tmax. Heat wave is a period of at least three or five consecutive days during which Tmax exceeds the long-term average by one or more standard deviations [39] or established amount of Celsius degrees (5 °C, [40]). In the last group of definitions, the threshold is based on the probability of occurrence of a particular Tmax. Often the 95th annual or summer percentile of Tmax is used and a heat wave is usually defined as a period of three or five consecutive days with Tmax exceeding this threshold [41–43]. Because the topic of this paper is heat waves that simultaneously cover a significant part of the country's surface, this third definition was adopted. A hot day is defined as a day with Tmax exceeding the 95th summer percentile of Tmax in the reference period 1961–1990 and a heat wave is defined as a period of at least three consecutive hot days. First, the 95th percentile of summer day (June, July, August) Tmax for the reference period 1961–1990 was calculated. This value was taken as the thermal threshold for hot days. Then days considered as hot days were selected where Tmax was equal to or greater than this threshold. A hot day in Poland was assumed to be a hot day at least at one station. In each year, the number of hot days and the number of hot station-days were counted. The annual number of station-days, *ST*, is calculated as

$$ST = \sum_{i=1}^N n_i$$

where *N* is the number of hot days in Poland in this year and *n<sub>i</sub>* is the number of stations on which the day *i* is a hot day (e.g., on a hot day at 5 stations, the number of hot station-days is 5). In order to assess the long-term variability, the linear trend of the number of hot days and hot station-days was calculated using the least squared method throughout the analyzed period (1951–2019) and after 1980 (1980–2019), when a significant increase in such days was observed. The trends in the number of hot days in individual stations were also calculated. The statistical significance of these trends was assessed with the Student's *t*-test. In order to assess the spatial extent of heat waves, the frequency of occurrence of hot days was counted depending on the number of stations where they were simultaneously observed. The distribution of hot days in individual months of the year was also examined, broken down into consecutive decades. The second goal was to determine the circulation conditions during long-lasting heat waves with a large spatial extent. Of all waves, the ones quoted simultaneously at least at 25% of stations (i.e., 10) and lasting not less than a week were selected. These waves were further analyzed.

The variables describing the circulation were the pressure at sea level (SLP), the geopotential of isobaric levels of 500 and 700 hPa, and the wind on both isobaric levels. The monthly mean values of all these variables in the period 1951–2019 were calculated in each grid of the studied area. SLP and geopotential anomalies were counted on each day of selected waves. Then, for each wave, the mean anomalies of these values were calculated and presented on maps. Average wind speed maps were also created in each wave. The obtained maps were compared and divided into groups differing in the location of the main baric centers.

Vertical velocity was used to describe the downward and upward motion of the air in the centers of highlands over Poland or in its vicinity. The average anomalies of vertical velocity in selected heat waves were calculated, as well as anomalies in the consecutive days of these waves, starting from the second day preceding and ending on the second day after their ends. On this basis, the dynamic of the development of anticyclonic systems responsible for the formation of the heat wave was analyzed.

All interpolations were performed in SUFRER using the kriging method.

### 3. Results

#### 3.1. Hot Days and Heat Waves

The 95th percentile of maximum daily temperature from summer months (JJA) in the reference period 1961–1990 is presented in Figure 2. The values range from 25.8 °C in Zakopane to 30.4 °C in Słubice and Poznań. Lower values were observed only in high mountain stations, 16.5 °C on Kasprowy Wierch (1991 m a.s.l.) and 18.0 °C on Śnieżka (1603 m a.s.l.). These percentiles were used as thermal thresholds for the hot day highlight. A day is considered as hot in Poland if it is hot in at least one station. The annual frequencies of hot days in Poland (Figure 3) are increasing. The linear trend throughout the analyzed period was 3.0 days/decade. After 1980, the trend significantly increased and amounted to 7 days/decade. The increase in the number of hot days was not even across Poland. It was much stronger in the south of the country than in the north. Throughout the analyzed period, the values ranged from 0.5 days/decade in Gorzów in the northwest to 2.4 days/decade in Rzeszów in the southeast (Figure 4a). After 1980, when the trend increased, it ranged from 0.4 days/decade in Kołobrzeg near the coast to 5.2 in Rzeszów in the southeast (Figure 4b).

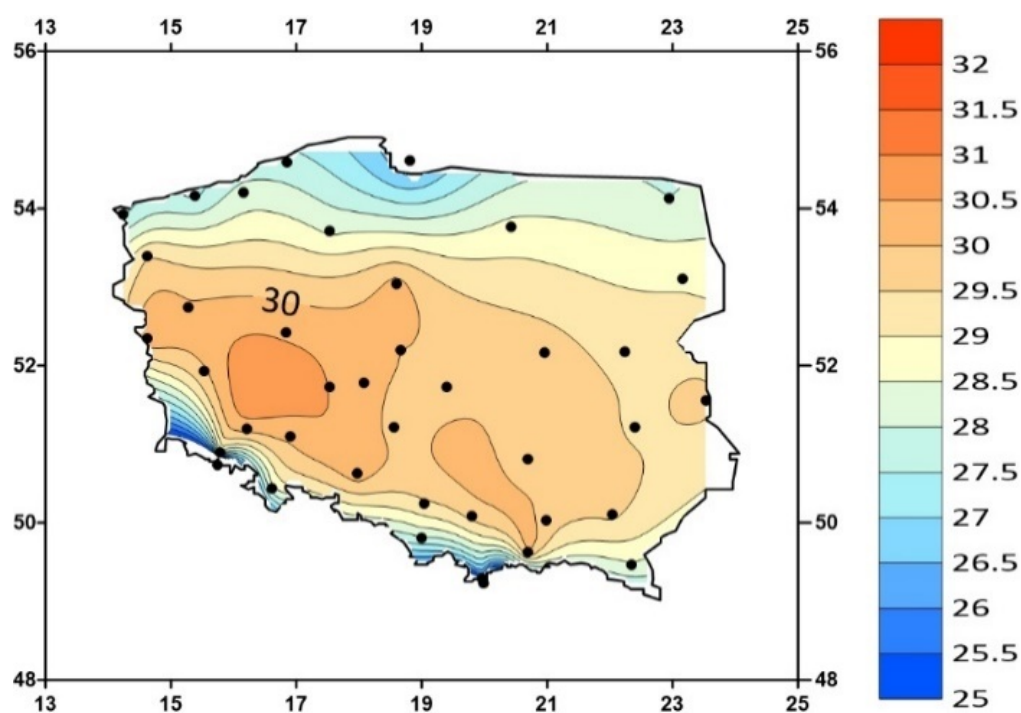


**Figure 2.** Spatial distribution of 95th percentile of daily maximum temperature on summer days (JJA) in the reference period 1961–1990.

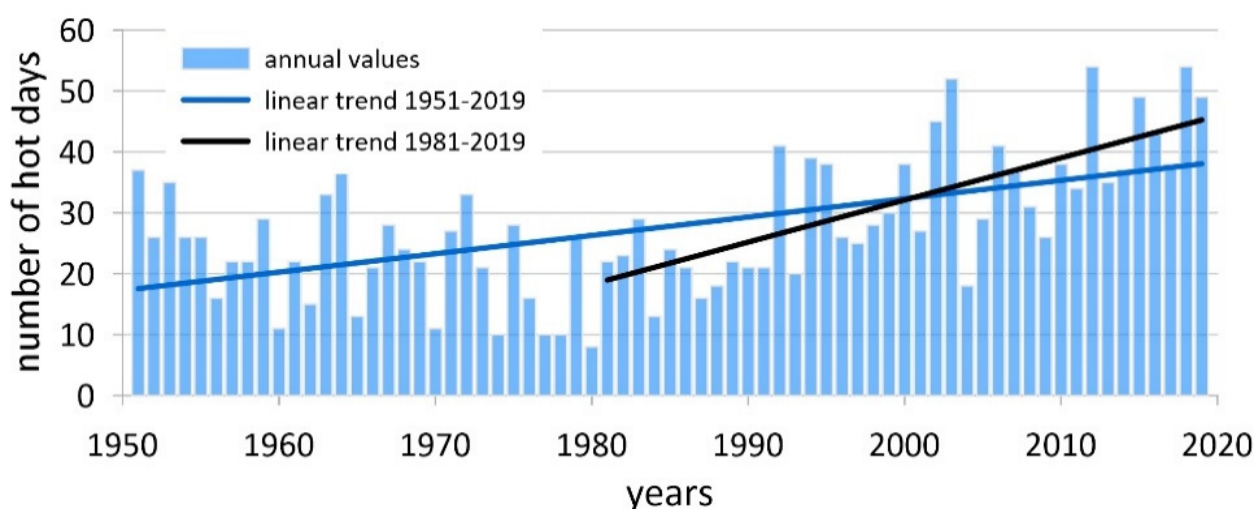


Figure 3. Annual frequencies of hot days in Poland in the period 1951–2019.

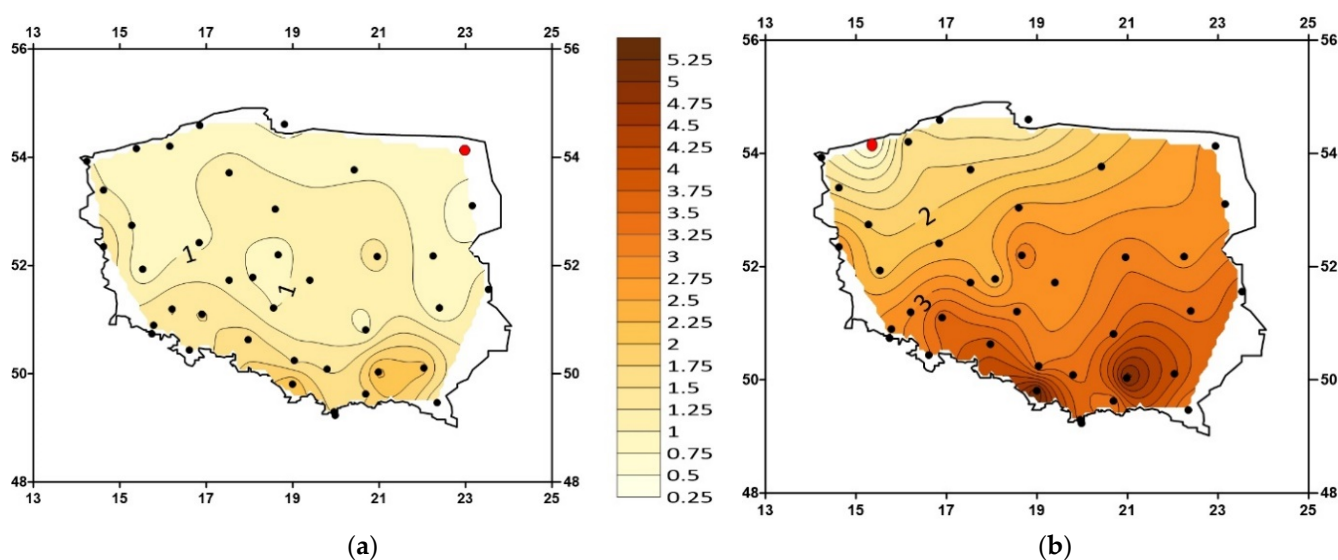
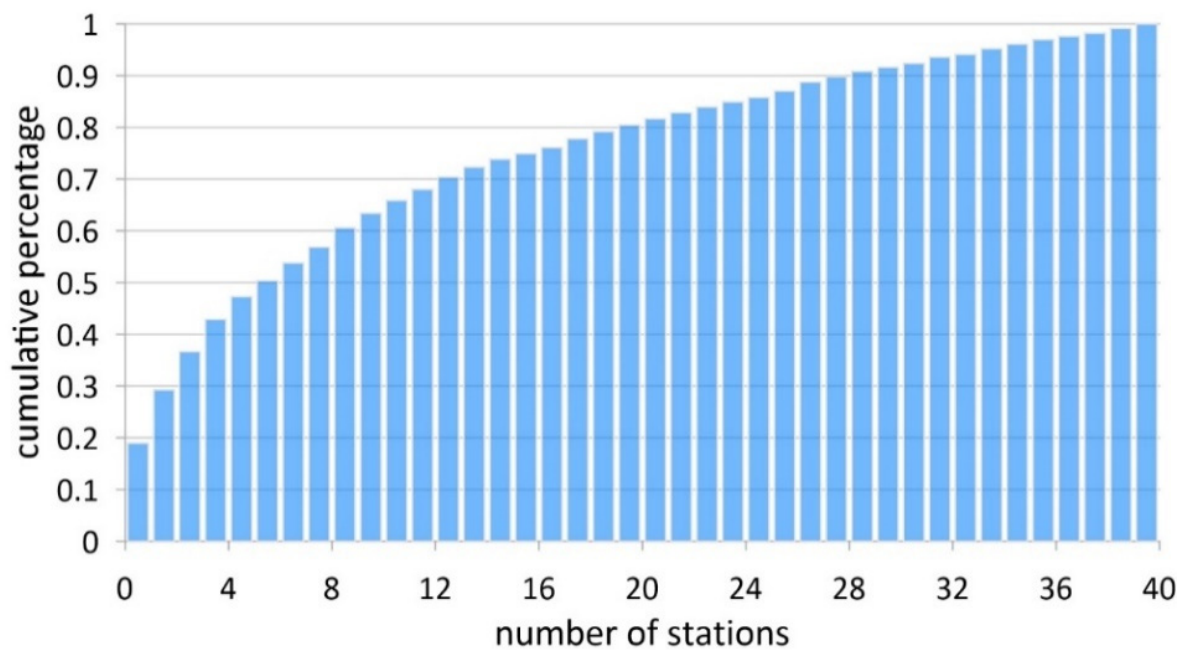


Figure 4. Linear trend coefficient in days/year of frequency of hot days in Poland: (a) in the period 1951–2019; (b) in the period 1980–2019. Red dots indicate points where trend is not significant at 0.05 level.

Out of all hot days in Poland, in almost 19% of cases, the thermal threshold was exceeded only at one station (Figure 5). During 50% of hot days, a heat threshold was exceeded at no more than eight stations. However, during 50% of hot days, the threshold was exceeded simultaneously on more than half of the stations surveyed.

In order to take into account the spatial extent of heat in Poland, the number of hot station-days was analyzed (Figure 6). The annual frequencies of heat station-days in Poland were increasing. The linear trend throughout the analyzed period was 48.8 station-days/decade. After 1980, the trend significantly increased and amounted to 110.7 station-days/decade.

On an annual basis, hot days may appear in Poland from April to October. In the first part of the analyzed period, they most often appeared in July, and slightly less frequently in August. In the past three decades, the proportions have reversed and more hot days were observed in August (Figure 7). The total number of hot days has also increased significantly, confirming a strong upward trend.



**Figure 5.** Cumulative relative frequencies of hot days in Poland in the period 1951–2019 observed simultaneously at given number of stations.

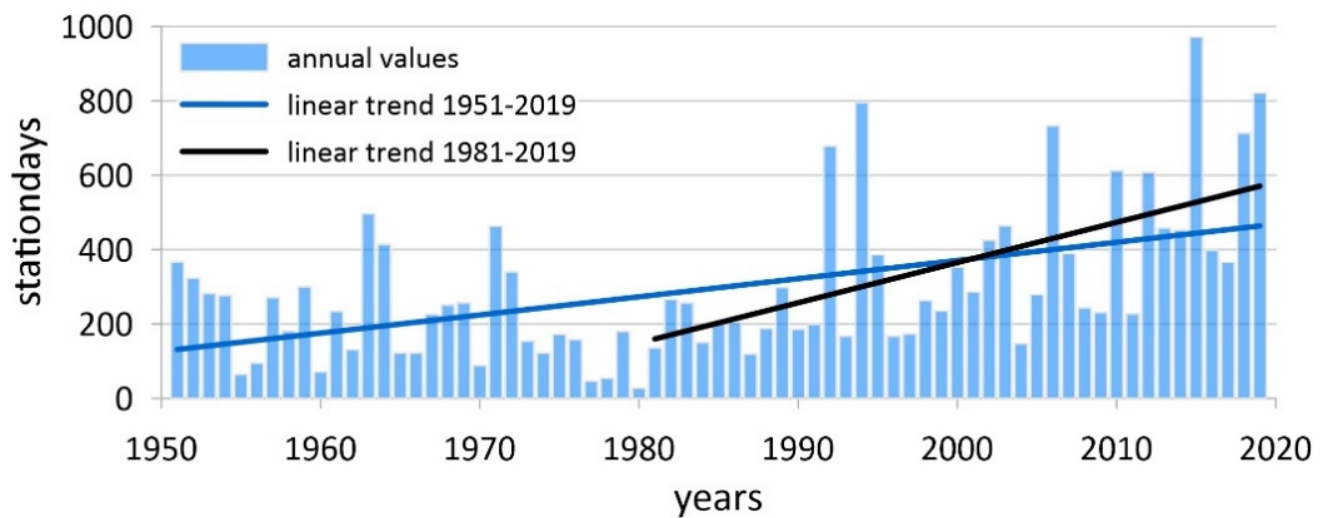


**Figure 6.** Annual frequencies of hot station-days in Poland in the period 1951–2019.

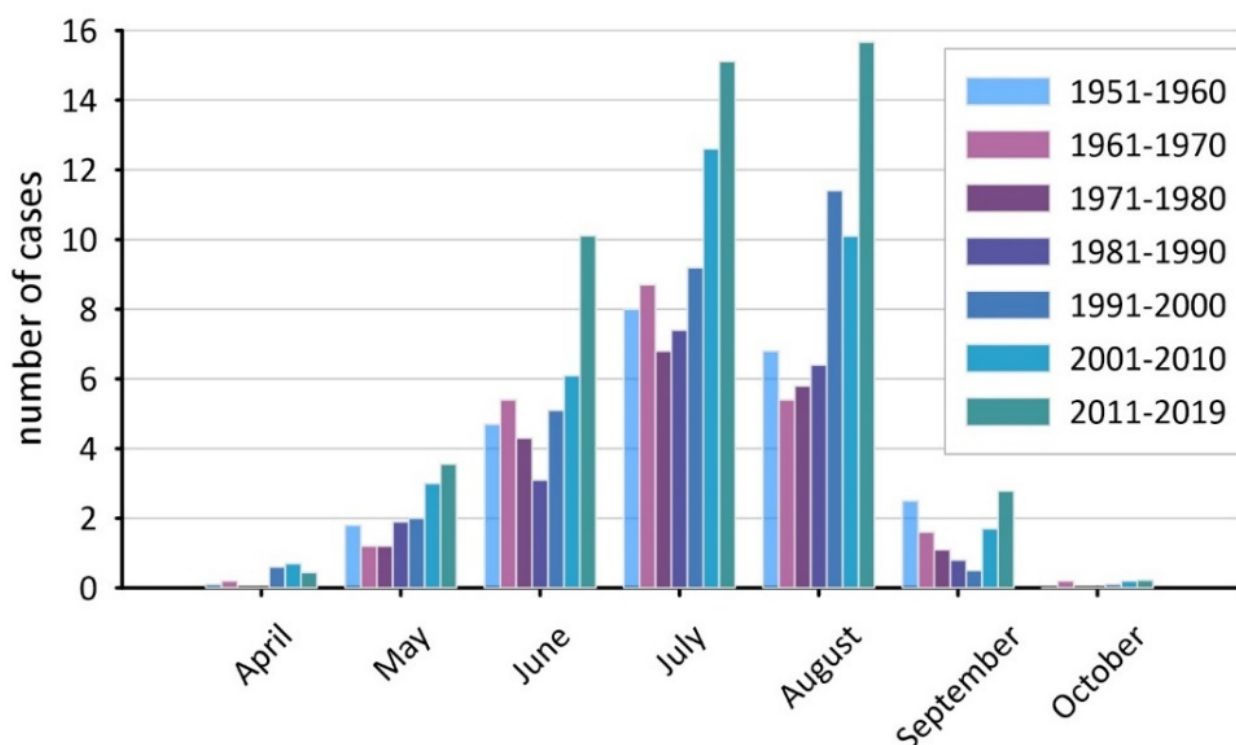


**Figure 7.** Average monthly numbers of hot days from April to October in the following decades.

In order to trace the circulation conditions conducive to the occurrence of heat waves in Poland, the longest heat waves were selected, during which the temperature exceeded the thresholds at least at 25% of analyzed stations (in this case, 10). Their list is presented in Table 1. Only 11 waves observed simultaneously at 10 stations lasted a week or more. Only one of them occurred in the first half of the analyzed period and six of them (more than half) occurred in the last decade. The two longest waves, 16 and 13 days long, happened in the 1990s. In July 2006, two heat waves occurred; they are further referred to as 2006a and 2006b. Four colder days separated them.

**Table 1.** The longest heat waves observed simultaneously at least at 10 stations in Poland.

Length of Wave in Days	Period	The Average Number of Stations
16	23.07–7.08 1994	32.5
13	30.07–11.08 1992	24.2
13	3–15.08 2015	31.5
12	18–29.07 2006	29.1
9	9–17.07 2010	31.2
9	5–13.07 2006	26.6
8	2–9.08 2013	22.8
8	28.07–4.08 2018	28.3
7	26.08–1.09 2019	29.6
7	30.07–5.08 2017	22.3
7	1–7.08 1963	31.1

Because there were two waves in 2006, the first (5–13.07) is further referred to as 2006a, and the other as 2006b.

### 3.2. Atmospheric Circulation during Selected Heat Waves

Circulation conditions during heat waves were studied on the basis of mean fields of the SLP, HGT500 and HGT700 anomalies, and wind fields on isobaric levels of 500 and 700 hPa (wind500 and wind700, respectively). As the HGT500 and HGT700 anomaly fields and wind500 and wind700 fields are very similar, only those for 700 hPa level are shown

on the maps. The 11 map sets, one for each wave listed in Table 1, can be broken down into four groups.

### 3.2.1. Group A

In the most common type of circulation on the  $60^{\circ}$  W– $60^{\circ}$  E section of the  $50^{\circ}$  N parallel, two systems of high pressure were observed; the main one over Scandinavia and northwestern Russia and the second, weaker one over the western Atlantic are shown in Figure 8. Two low-pressure systems were observed also: the main one over the eastern Atlantic and the second, slightly weaker one over eastern Europe (Figure 8a). The low pressure was also observed over the Mediterranean Sea. The SLP anomalies ranged from slightly below  $-5$  to above  $5$  mb. The geopotential anomalies of the 700 hPa level surface ranged from  $-100$  to  $150$  m (Figure 8b). Figure 8c shows that over the Atlantic in latitudes  $40$ – $60^{\circ}$  N at the level of 700 and 500 hPa, there was a strong zonal circulation with the southern component both in the western part, off the coast of North America, and the eastern part, off the coast of Europe. In eastern Europe, the northern or northwestern wind was observed. In Poland, southwestern winds occurred over the western part and northeastern over the eastern part. This circulation type prevailed during four heat waves listed in Table 1, in the years 1994, 2010, 2015, and 2018. Cases from 1994 and 2015 were described in detail by Tomczyk et al. [44]. Figure 8 shows the SLP and HGT700 anomaly map and wind700 fields for the 1994 wave. Maps for the remaining cases are included in the Supplement (Figures S1–S3).

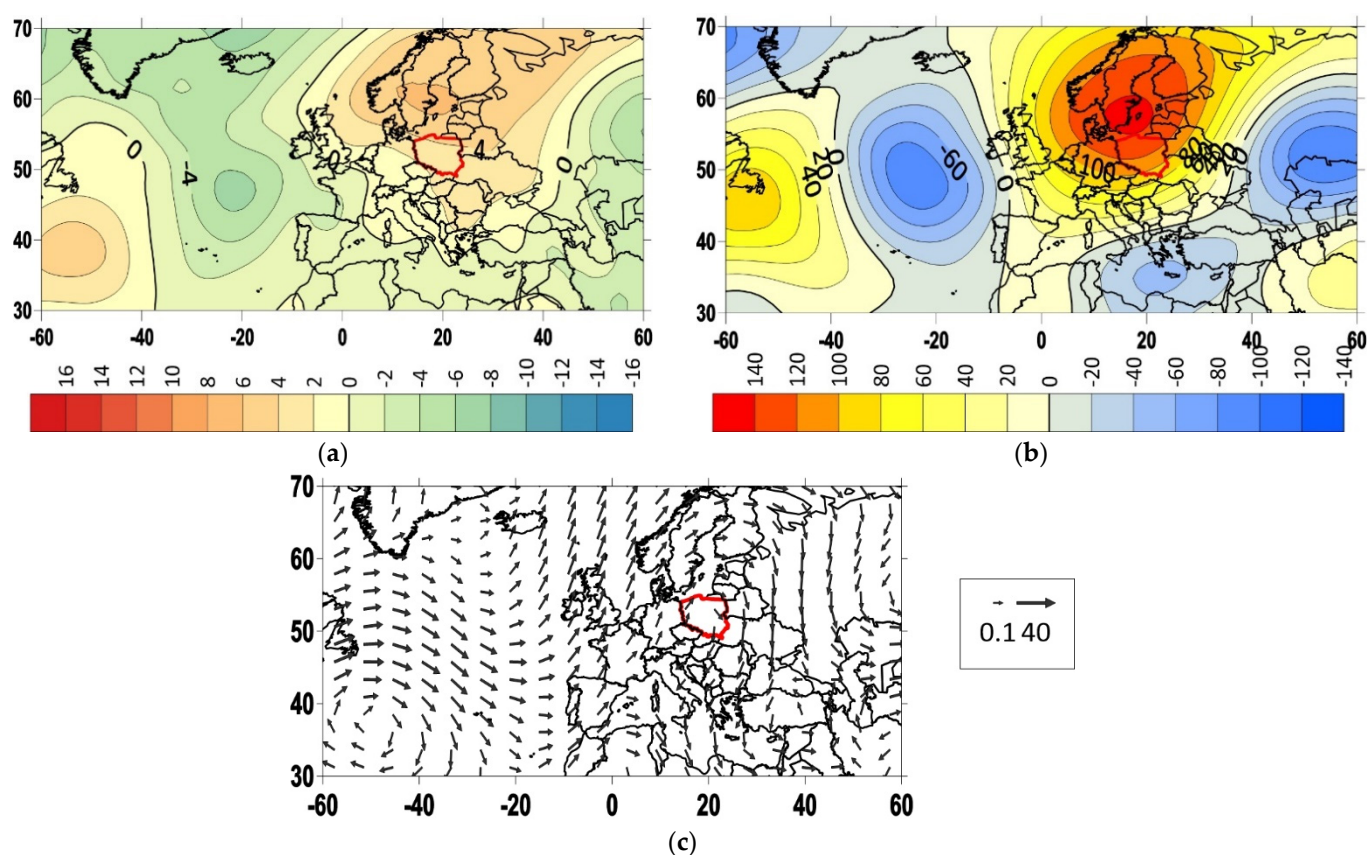


**Figure 8.** Average fields for the 1994 heat wave: (a) anomalies of SLP; (b) anomalies of HGT700 mb; (c) wind at 700 hPa level. The red line marks the borders of Poland.

### 3.2.2. Group B

In the second group of cases, the high-pressure ridge extended across the Atlantic in the 30–50° N belt and Europe (Figure 9a). There was a clear maximum in pressure anomaly slightly to the east of Poland, sometimes exceeding 10 mb. The second, smaller maximum was located in the area of the climatic location of the Azorian High. A low-pressure system was observed near Iceland. Figure 9b shows that the maximum of the positive anomalies of 700 hPa geopotential level was observed close to the eastern boundary of Poland and exceeded 120 m. The highest negative anomalies were located close to Iceland and exceeded 100 m. Negative anomalies were observed also over the eastern part of the Mediterranean Sea. Over the Atlantic in latitudes 40–60° N at the level of 700 and 500 hPa, there was a strong zonal circulation. Figure 9c shows that over Europe, the wind obtained the small southern component. In Poland, southwestern winds occurred. This circulation type prevailed during three heat waves listed in Table 1, in the years 1992, 2006 (wave 2006a), and 2017. Figure 9 shows the SLP and HGT700 anomaly map and wind700 fields for the 2006a wave. Maps for the remaining cases are included in the Supplement (Figures S4 and S5).

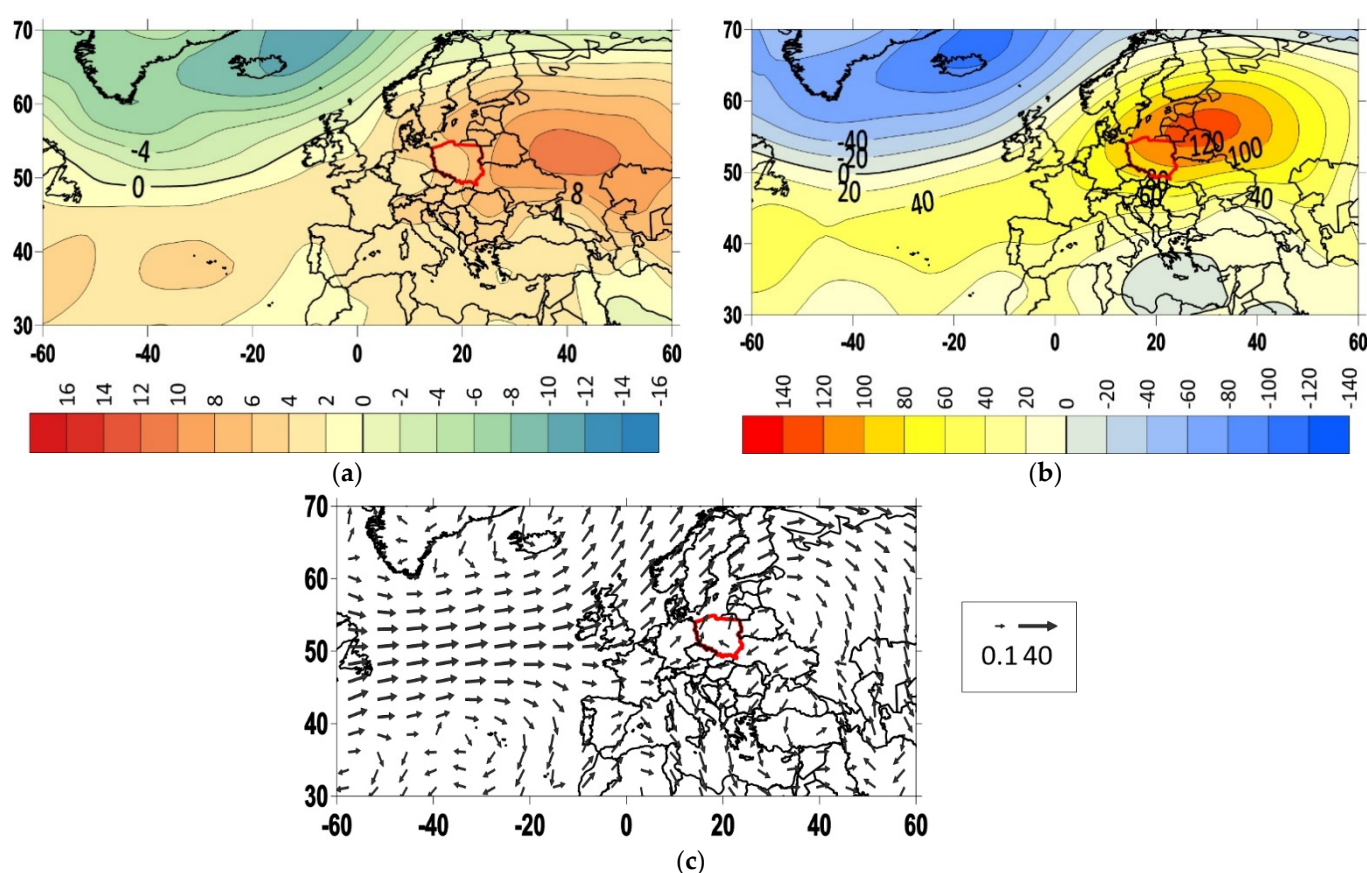


**Figure 9.** Average fields for the 2006a heat wave: (a) anomalies of SLP; (b) anomalies of HGT700 mb; (c) wind at 700 hPa level. The red line marks the borders of Poland.

### 3.2.3. Group C

In the third group of cases, the high-pressure ridge stretched meridionally across Europe in the 0–40° E belt and went north to the Arctic (Figure 10a). There was a clear maximum in pressure anomaly slightly to the north of Poland, sometimes exceeding 5 mb. Two low-pressure systems were observed on the east and west of the high-pressure ridge. The western low was centered on the Northern Atlantic on the northwest of the British Isles. The eastern low was centered over the European part of Russia. Figure 10b shows that the maximum of the positive anomalies of 700 hPa geopotential level was observed

close to the southern Baltic Sea and exceeded 120 m. The highest negative anomalies were located close to Iceland and exceeded 100 m. Negative anomalies over Russia were of similar intensity. Figure 10c shows that over the Atlantic in latitudes 40–60° N at the level of 700 and 500 hPa, there was a strong zonal circulation. Over the western part of Europe, the wind obtained the southern component and over eastern Europe, the northern winds dominated. In Poland, southwestern winds occurred. This circulation type prevailed during three heat waves listed in Table 1, in the years 2006 (wave 2006b), 2013, and 2019. Figure 10 shows the SLP and HGT700 anomaly map and wind700 fields for the 2019 wave. Maps for the remaining cases are included in the Supplement (Figures S6 and S7).

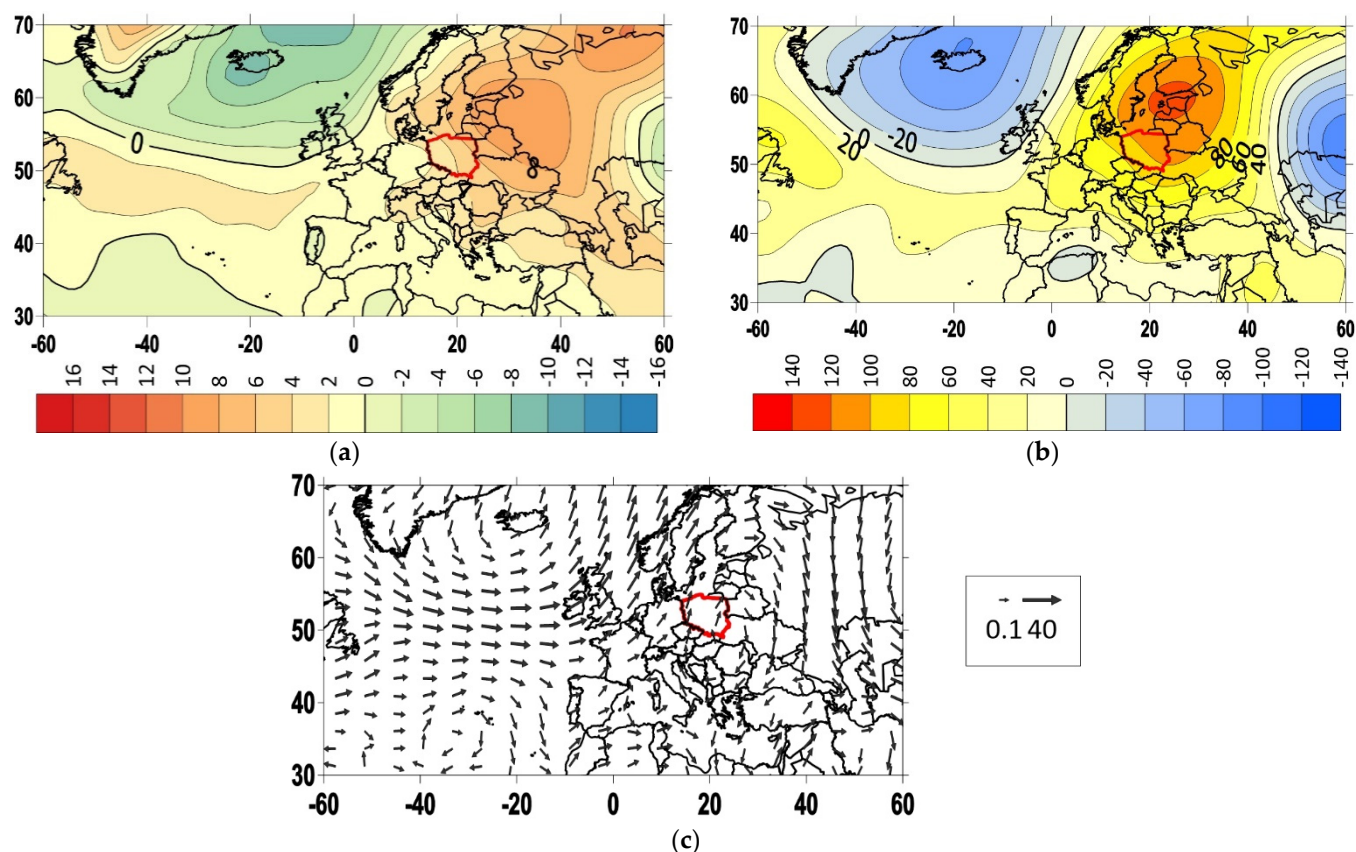


**Figure 10.** Average fields for the 2019 heat wave: (a) anomalies of SLP; (b) anomalies of HGT700 mb; (c) wind at 700 hPa level. The red line marks the borders of Poland.

### 3.2.4. Group D

The wave of 1963 was clearly different from the others (Figure 11). Figure 11a shows that the higher than normal pressure occurred in almost all of the North Atlantic, Scandinavia, and the part of Europe that lies to the east of Poland. Highest anomalies exceeded 5 mb. Over western, central, and southern Europe, negative SLP anomalies were observed; the highest anomalies also exceeded 5 mb. Poland was located on the boundary between these two areas and the izoanomaly 0 ran through its northern part. Figure 11b shows that the maximum of the positive anomalies of 700 hPa geopotential level was observed on the eastern edges of Europe and in Scandinavia and reached 100 m. The secondary maximum was over the central part of the Northern Atlantic, slightly south of 50° N, and was about 50 m. The highest negative anomalies were located over northern Spain and the Bay of Biscay and were about 50 m. The negative anomalies over Asia Minor and the eastern edges of Europe were of similar intensity. Over the Atlantic, zonal circulation at the level of 700 and 500 hPa was only in latitudes 50–60° N (Figure 11c). Over the western part of

Europe, the wind had a strong southern component, and over eastern Europe, the northern winds dominated. In Poland, southern winds occurred.

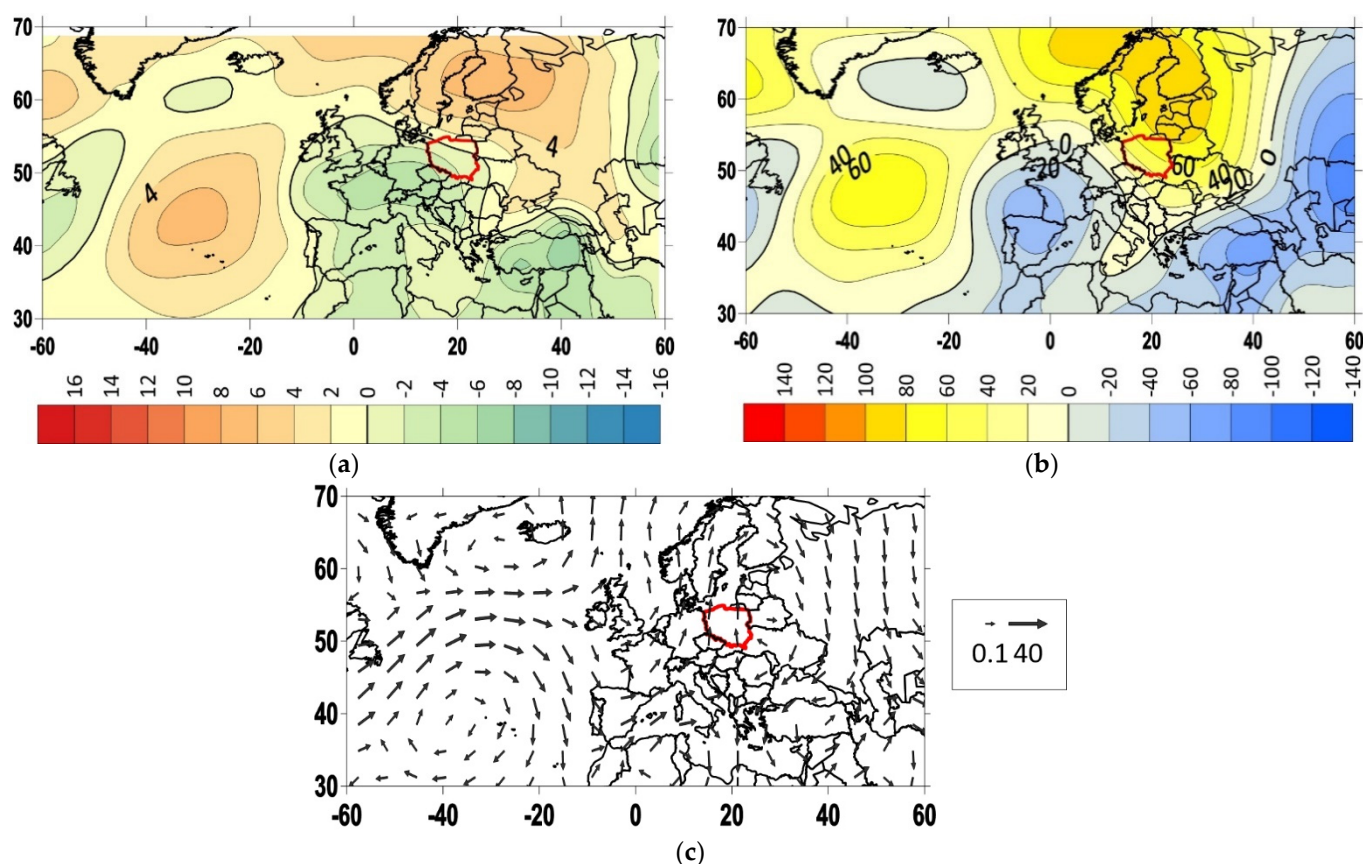


**Figure 11.** Average fields for the 1963 heat wave: (a) anomalies of SLP; (b) anomalies of HGT700 mb; (c) wind at 700 hPa level. The red line marks the borders of Poland.

### 3.3. Vertical Velocity

Vertical velocity  $\omega$  (omega) used in this paper is expressed in pressure coordinates and defined as  $dp/dt$ , where  $p$  means pressure and  $t$  means time. A positive omega means that the velocity is directed toward the Earth and it occurs in the subsidence zone. A negative omega is in an upward motion zone. In this section, the anomalies of vertical velocity during heat waves are analyzed. Positive anomalies are often induced by the anticyclonic circulation. They can be accompanied by clear sky, drier air, and soil moisture deficiency causing the air temperature to rise [31]. Here, for each heat wave described in the previous section, the average vertical velocity anomaly over the duration of the wave will be shown, as well as daily vertical velocity anomaly values before, during, and after the heat wave.

#### 3.3.1. Group A

During the 1994 heat wave, average vertical velocity anomaly values were positive in Scandinavia and Central Europe, that is, in the area covered by the high-pressure system (Figure 12a). Positive values were observed here on a day before the heat wave, when the anticyclone strengthened, and in the first half of the heat wave duration (Figure 12b,c). However, this was followed by the stabilization phase, when the vertical velocity anomalies in this region were close to zero. Then the anomalies became negative, an upward motion appeared, the anticyclone weakened, and with it the heat wave ended (Figure 12d,e).

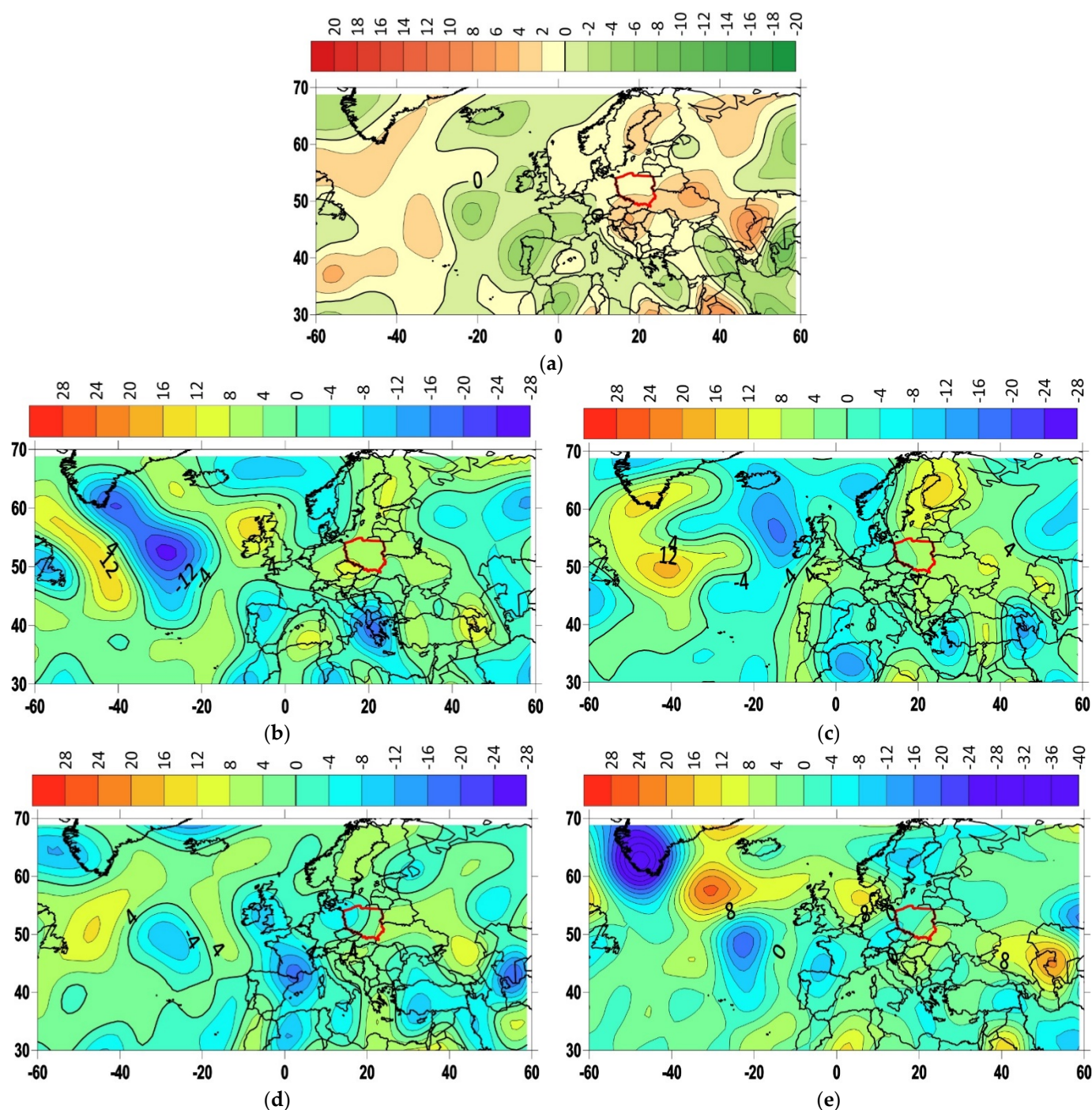


**Figure 12.** Vertical velocity in  $10^{-2} \text{ Pa} \cdot \text{s}^{-1}$  for 1994 heat wave: (a) average in the period 23.07–7.08; (b) on day before heat wave (22.07); (c) on 25.07; (d) on 1.08; (e) on 6.08. The red line marks the borders of Poland.

### 3.3.2. Group B

In the 2006a heat wave, average vertical velocity anomaly values were positive in Poland, Ukraine, Belarus, and western parts of Russia as previously in the area covered by the high-pressure system (Figure 13a). Positive values were observed here on a day before the heat wave, when the anticyclone strengthened, and in the first half of the heat wave duration (Figure 13b,c). However, this was followed by the stabilization phase, when the vertical velocity anomalies in this region were close to zero. Then the anomalies became negative, an upward motion appeared, and the anticyclone on the east of Poland

disappeared and created a new one on the North Sea and the Danish Straits. The heat wave ended (Figure 13d,e).

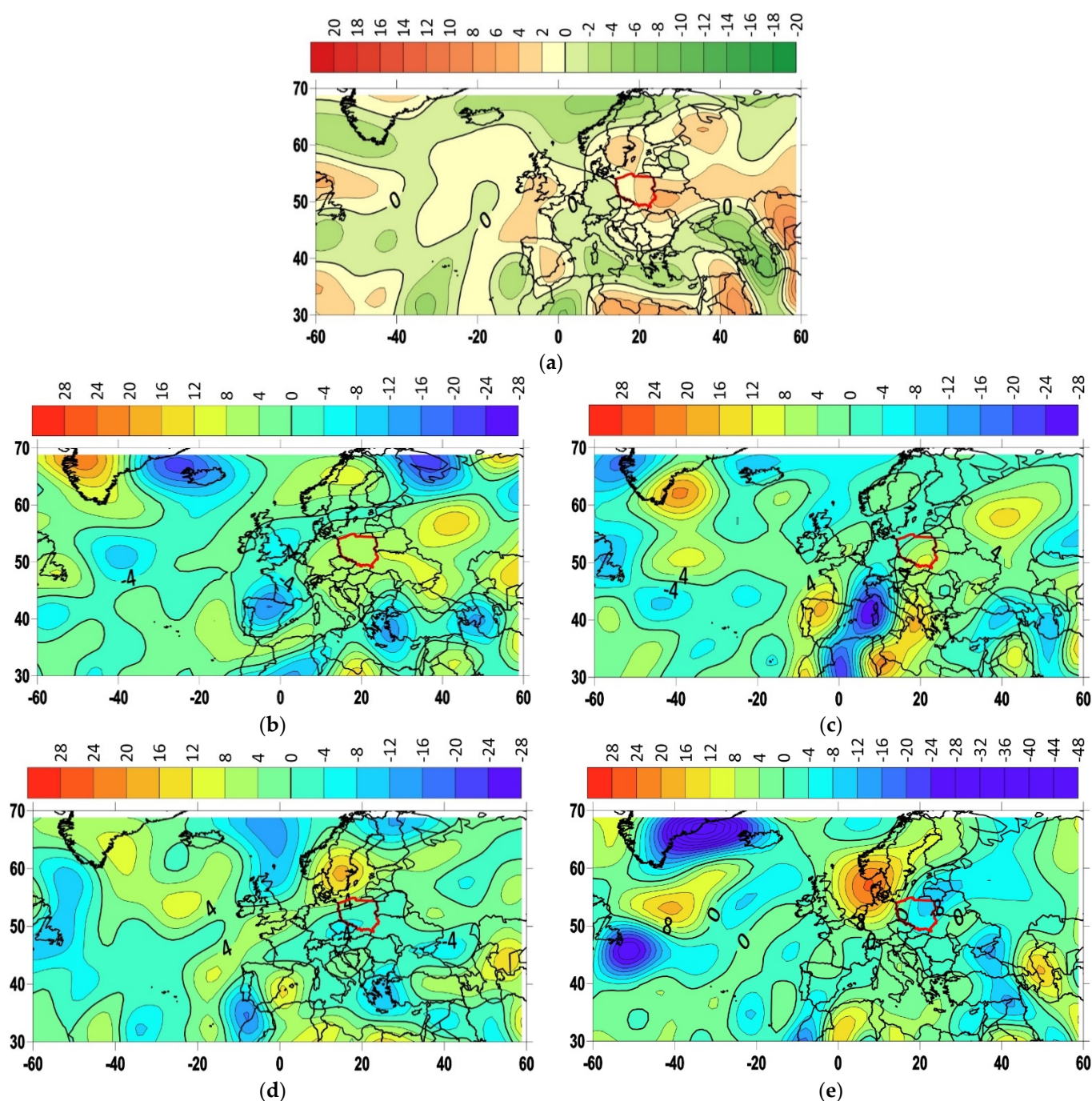


**Figure 13.** Vertical velocity in  $10^{-2} \text{ Pa} \cdot \text{s}^{-1}$  for 2006a heat wave: (a) average in the period 5–13.07; (b) on day before heat wave (4.07); (c) on 6.07; (d) on 12.07; (e) on day after heat wave (14.07). The red line marks the borders of Poland.

### 3.3.3. Group C

Average vertical velocity anomaly values were positive over almost all Europe, and in the narrow belt over Atlantic a little south of the  $50^\circ \text{ N}$  parallel (Figure 14a). Before and during the first days of the wave, unlike in the previous cases, the subsidence zone (the area of positive omega anomaly values) was located east of the center of the high-pressure system and not directly in the area of its deposition (Figure 14b,c). Positive values were

observed here in the second part of the heat wave duration. On a day after the heat wave, the anomalies became negative, an upward motion appeared, the anticyclone disappeared, and with it the heat wave ended (Figure 14d,e).

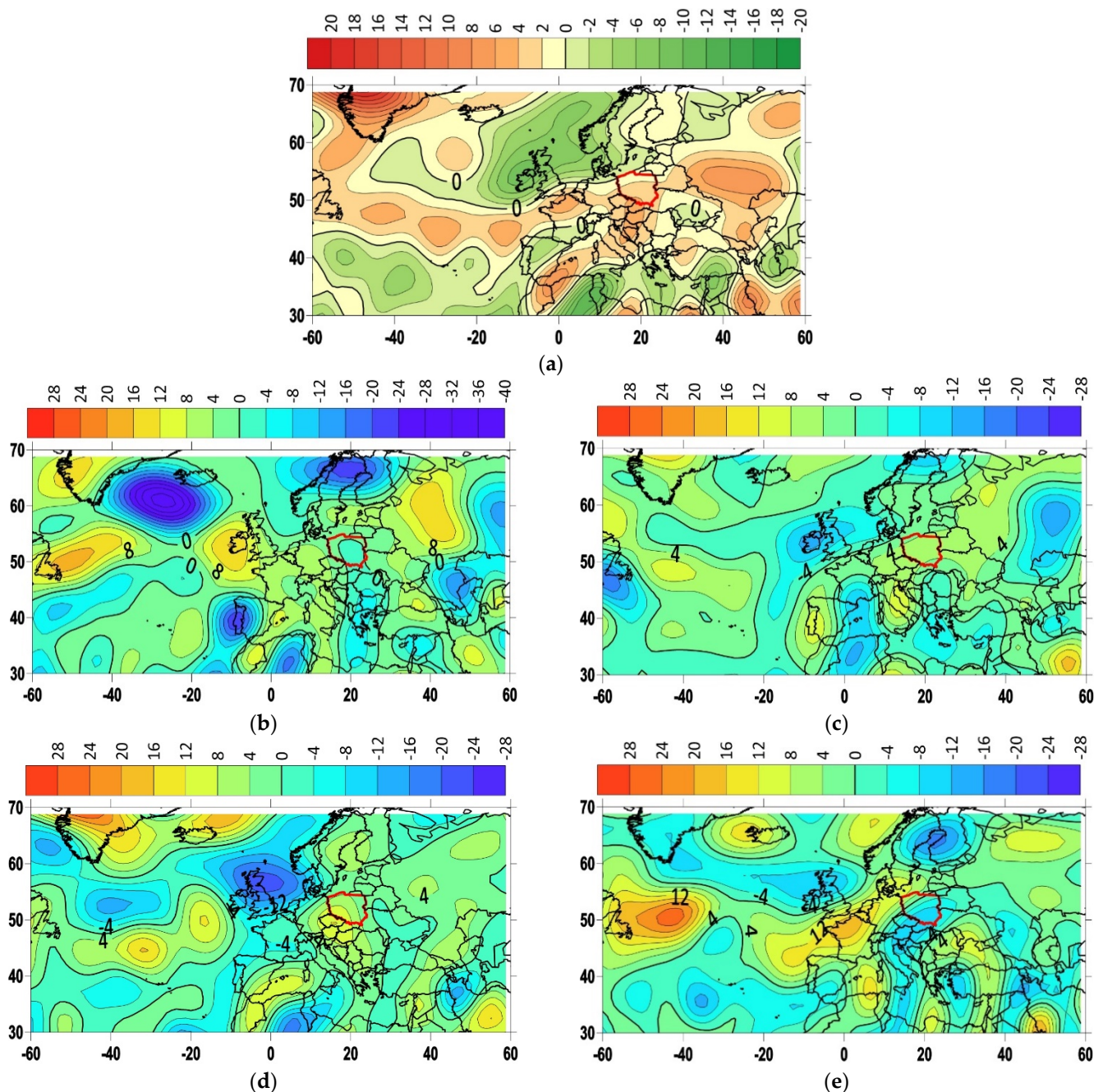


**Figure 14.** Vertical velocity in  $10^{-2} \text{ Pa} \cdot \text{s}^{-1}$  for 2019 heat wave: (a) average in the period 26.08–1.09; (b) on day before heat wave (25.08); (c) on 27.08; (d) on 31.08; (e) on day after heat wave (2.09). The red line marks the borders of Poland.

### 3.3.4. Group D

Average vertical velocity anomaly values were positive in Scandinavia, Central Europe, and western Russia, with the highest values in the northern part of the Baltic Sea and in the south and southeast of Poland (Figure 15a). A similar pattern was observed just before and in the first part of the heat wave (Figure 15b,c). It was followed by the stabilization phase, when the vertical velocity anomalies in this region were close to zero. Then the anomalies

became negative, an upward motion appeared, the anticyclone weakened, and with it the heat wave ended (Figure 15d,e).

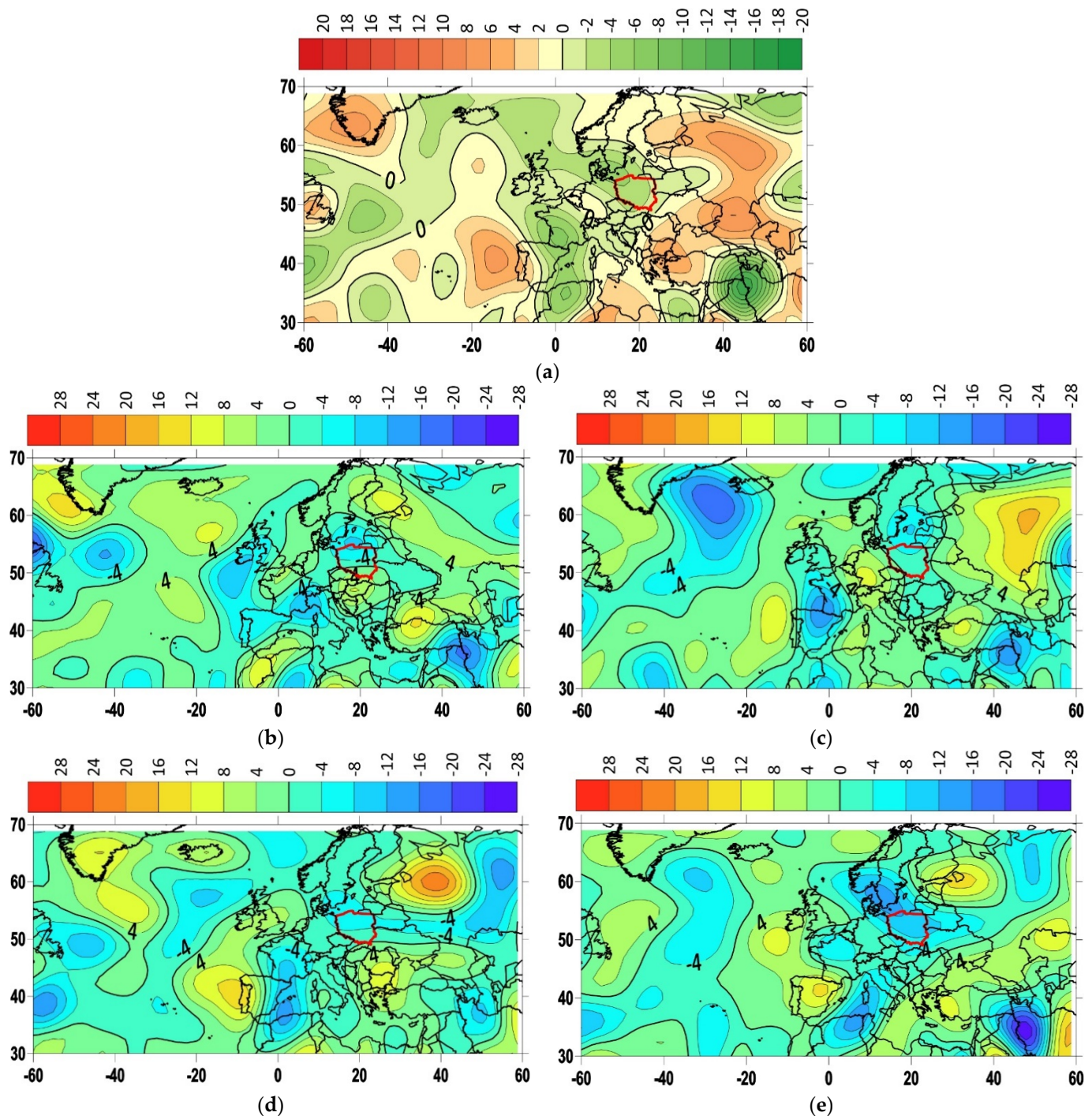


**Figure 15.** Vertical velocity in  $10^{-2} \text{ Pa} \cdot \text{s}^{-1}$  for 1963 heat wave: (a) average in the period 1–7.08; (b) on day before heat wave (31.07); (c) on 2.08; (d) on 6.08; (e) on day after heat wave (8.08). The red line marks the borders of Poland.

#### 4. Discussion

Together with upward trend in temperature, the changes in the number and persistence of hot days and heat waves in Poland were observed by many authors. The first findings were based on data from a few stations [8] or in a specific region [25,42,45]. In the others, the trends in hot days or heat waves were analyzed in the area of Central Europe,

of which Poland is only a part, and therefore a small number of Polish stations were taken into consideration [26]. In all cases, the trend in frequency and intensity of hot days and heat waves became more visible as the data series extended into the 21st century. This work used a dense network of stations and extended series until the end of 2019. A strict criterion for distinguishing hot days was adopted as days with  $T_{\max}$  exceeding the 95th percentile of  $T_{\max}$  from summer days (June, July, and August). This is a stronger condition than in some previous studies, where the 95th percentile of  $T_{\max}$  for the whole was taken [26], but weaker than in some others, where the  $30^{\circ}\text{C}$  threshold was used [45]. Nevertheless, the increase in the number of hot days, both in Poland and at individual stations and in hot station-days, turned out to be statistically significant everywhere. There has been a very strong increase in the number of hot days after 1980, especially in the last three decades. This increase was stronger in the south of Poland than in the north. Such tendencies (stronger increase in  $T_{\max}$  in summer in the south than in the north) were indicated also in the results of Wypych et al. [46] and Kejna and Rudzki [47]. However, it should be emphasized that the increasing frequency of hot days is not necessarily accompanied by an increase in absolute  $T_{\max}$  maxima. This means that the  $T_{\max}$  distribution has changed, which may be worth a more detailed analysis. It is also worth emphasizing that despite the use of a stronger criterion for distinguishing hot days, they were still recorded from April to October, as was shown by a milder criterion (95th percentile of  $T_{\max}$  for the whole year [26]). In the last three decades, the maximum occurrence of hot days has shifted from July to August. Previously, the maximum in August was only documented at stations near the coast [26]. This change may indicate the oceanization of Poland's climate, because in maritime climates, the period of the highest temperature moves from July to August.

Four types were distinguished when examining the atmospheric circulation during the period of extensive and long-lasting heat waves. During the first of them (Group A, Figures 8 and 12), the close to normal SLP and below normal HGT700 over southern Europe indicate that the air temperature in this part of the continent is below normal. Over Scandinavia and central Europe, a high-pressure pattern dominates with positive values of  $\omega$  making the sky clear and the air relatively dry. This contributes to high temperature in this region. This type occurred in 4 out of 11 analyzed heat waves. Therefore, it can be called dominant.

In the second type (group B, Figures 9 and 13), the center of the main high-pressure pattern is located over western Russia (Figure 9a) and extends far into the east. The center of the corresponding anticyclone at 700 hPa level is shifted on the west (Figure 9b) which means that the system is under development. This is confirmed by a vast area of air mass subsidence over central, northern, and eastern Europe (Figure 13a). Advection of air from the southeast and south, clear sky, and relatively dry air because of subsidence contribute to high temperature in Poland. The close to normal SLP and below normal HGT700 over southeastern Europe indicate that the air temperature in this part of the continent is below normal. This type occurred in 3 out of 11 analyzed heat waves.

In the third type (group C, Figures 10 and 14), the center of the main high-pressure pattern is also located over western Russia (Figure 10a), but its extent to the east is limited by the intensive low-pressure system. On the 700 hPa level, both patterns are strong and their centers are shifted on the west of the appropriate patterns on SLP maps (Figure 10b). On Figure 14a, a distinct belt of air masses subsidence around the parallel  $50^{\circ}\text{N}$  runs through Europe from France to western Russia. Advection of air from the southeast and south, clear sky, and relatively dry air because of subsidence contribute to high temperature in Poland. The close to normal SLP and below normal HGT700 over southwestern Europe indicate that the air temperature in this part of the continent is below normal. This type occurred in 3 out of 11 analyzed heat waves.

The fourth type (group D, Figures 11 and 15) occurred in 1963. On the SLP map (Figure 11a) it can be seen that Poland is located in the transitional area between the low-pressure system with the center above southern Germany and high-pressure system with the center above northern Scandinavia. At 700 hPa level, the center of the low is shifted

over the Biscay Bay and the high-pressure system has the center over central Scandinavia (Figure 11b). These systems are accompanied by the vast area of air mass subsidence over northern, northeastern, and central Europe (Figure 15a). Advection of air from the south, clear sky, and relatively dry air because of subsidence contribute to high temperature in Poland. This type occurred only once, at the beginning of the analyzed period, and did not repeat in the post-1980 warming period.

Tomczyk and Bednorz [26] distinguished only three circulation types accompanying heat waves. Here their type with the anticyclone over Scandinavia was divided into two: group A and D. Both types are similar over the European continent but significantly different over the northern Atlantic. They are also different in southern Europe. In type A, the air temperature in the Mediterranean region is slightly below normal and it is not a case of type D. Four synoptic patterns were also distinguished previously by Wibig [27]. Although many studies point to the relationship between heat waves and blocking situations [26,27,44,48], over the Atlantic in all cases, a strong zonal flow and a greater than average pressure gradient is observed. However, the wind turns over the continent and in central Europe the dominant direction is southwest or south.

The study of vertical velocity in conjunction with the analysis of synoptic situations conducive to the formation of heat waves is quite new [31]. As the dynamic of the phenomenon is clearly visible, it seems that it can be a useful tool. In the future, it should be combined with soil moisture, cloudiness, and outgoing longwave radiation measures.

## 5. Conclusions

The most important results of the paper should be mentioned:

- The frequency of hot days increased significantly
- After 1980, the rate of increase in the frequency of heat waves significantly accelerated
- Heat waves may appear from April to October
- During the last decade, more than half of all extensive and long-lasting heat waves that occurred in Poland after 1950 were observed
- The circulation patterns favoring the appearance of heat waves differ, but in most cases, anticyclone is present over Poland or in its vicinity
- Spatial and temporal distribution of vertical velocity anomalies allows distinguishing clear phases of strengthening, stabilization, and weakening of anticyclone accompanying the occurrence of a heat wave

Results obtained using the vertical velocity suggest that it would be worth using outgoing longwave radiation (OLR) data to study the dynamics of heat wave development.

**Supplementary Materials:** The following are available online at <https://www.mdpi.com/2073-4433/12/3/340/s1>, Figure S1: Average fields for the 2010 heat wave: (a) anomalies of SLP; (b) anomalies of HGT700 mb; (c) wind at 700 hPa level, Figure S2: Average fields for the 2015 heat wave: (a) anomalies of SLP; (b) anomalies of HGT700 mb; (c) wind at 700 hPa level, Figure S3: Average fields for the 2018 heat wave: (a) anomalies of SLP; (b) anomalies of HGT700 mb; (c) wind at 700 hPa level, Figure S4: Average fields for the 1992 heat wave: (a) anomalies of SLP; (b) anomalies of HGT700 mb; (c) wind at 700 hPa level, Figure S5: Average fields for the 2017 heat wave: (a) anomalies of SLP; (b) anomalies of HGT700 mb; (c) wind at 700 hPa level, Figure S6: Average fields for the 2006b heat wave: (a) anomalies of SLP; (b) anomalies of HGT700 mb; (c) wind at 700 hPa level, Figure S7: Average fields for the 2013 heat wave: (a) anomalies of SLP; (b) anomalies of HGT700 mb; (c) wind at 700 hPa level.

**Funding:** This research received no external funding.

**Institutional Review Board Statement:** Not applicable.

**Informed Consent Statement:** Not applicable.

**Data Availability Statement:** No new data was created in this study.

**Acknowledgments:** The author would like to thank IMWM-NRI for providing the temperature data and NCEP/NCAR archives for Reanalysis 1 data used in this study.

**Conflicts of Interest:** The authors declare no conflict of interest.

## References

1. IPCC. *Climate Change 2013: The Physical Science Basis. Contribution of Working Group I to the Fifth Assessment Report of the Intergovernmental Panel in Climate Change*; Cambridge University Press: Cambridge, UK, 2013.
2. WMO Statement on the State of the Global Climate in 2019; WMO-No 1248; World Meteorological Organization: Geneva, Switzerland, 2020.
3. Changnon, S.A.; Kunkel, K.E.; Reinke, B.C. Impacts and responses to the 1995 heat wave: A call to action. *Bull. Am. Meteorol. Soc.* **1996**, *77*, 1497–1506. [\[CrossRef\]](#)
4. De Bono, A.; Giuliani, G.; Kluser, S.; Peduzzi, P. Impacts of summer 2003 heat wave in Europe. *Eur. Environ. Alert Bull.* **2004**, *2*, 1–4.
5. Karl, T.R.; Knight, R.W. The 1995 Chicago heat wave: How likely is a recurrence? *Bull. Am. Meteorol. Soc.* **1997**, *78*, 1107–1119. [\[CrossRef\]](#)
6. Vandentorren, S.; Suzan, F.; Medina, S.; Pascal, M.; Maulpoix, A.; Cohen, J.-C.; Ledrans, M. Mortality in 13 French cities during the August 2003 heat wave. *Am. J. Public Health* **2004**, *94*, 1518–1520. [\[CrossRef\]](#) [\[PubMed\]](#)
7. Kysely, J. Temporal fluctuations in heat waves at Prague–Klementinum, the Czech Republic, from 1901–1997, and their relationships to atmospheric circulation. *Int. J. Climatol.* **2002**, *22*, 33–50. [\[CrossRef\]](#)
8. Wibig, J.; Podstawczyńska, A.; Rzepa, M.; Piotrowski, P. Heatwaves in Poland—Frequency, trends and relationships with atmospheric circulation. *Geogr. Pol.* **2009**, *82*, 33–46. [\[CrossRef\]](#)
9. Kysely, J. Recent severe heat waves in central Europe: How to view them in a long-term prospect? *Int. J. Climatol.* **2010**, *30*, 89–109. [\[CrossRef\]](#)
10. Beniston, M. The 2003 heat wave in Europe: A shape of things to come? An analysis based on Swiss climatological data and model simulations. *Geophys. Res. Lett.* **2004**, *31*, L02202. [\[CrossRef\]](#)
11. Black, E.; Blackburn, M.; Harrison, G.; Hoskins, B.; Methven, J. Factors contributing to the summer 2003 European heatwave. *Weather* **2004**, *59*, 217–223. [\[CrossRef\]](#)
12. Zaitchik, B.F.; Macalady, A.K.; Bonneau, L.R.; Smith, R.B. Europe’s 2003 heat wave: A satellite view of impacts and land-atmosphere feedbacks. *Int. J. Climatol.* **2006**, *26*, 743–769. [\[CrossRef\]](#)
13. Barriopedro, D.; Fischer, E.M.; Luterbacher, J.; Trigo, R.M.; García-Herrera, R. The hot summer of 2010: Redrawing the temperature record map of Europe. *Science* **2011**, *332*, 220–224. [\[CrossRef\]](#) [\[PubMed\]](#)
14. Dole, R.; Hoerling, M.; Perlwitz, J.; Eischeid, J.; Pegion, P.; Zhang, T.; Quan, X.W.; Xu, T.; Murray, D. Was there a basis for anticipating the 2010 Russian heat wave? *Geophys. Res. Lett.* **2011**, *38*, L06702. [\[CrossRef\]](#)
15. Grumm, R.H. The Central European and Russian heat event of July–August 2010. *Bull. Am. Meteorol. Soc.* **2011**, *92*, 1285–1296. [\[CrossRef\]](#)
16. Otto, F.E.L.; Massey, N.; van Oldenborgh, G.J.; Jones, R.G.; Allan, M.R. Reconciling two approaches to attribution of the 2010 Russian heat wave. *Geophys. Res. Lett.* **2012**, *39*, L04702. [\[CrossRef\]](#)
17. Duchez, A.; Frajka-Williams, E.; Josey, S.A.; Evans, D.G.; Grist, J.P.; Marsh, R.; McCarthy, G.D.; Sinha, B.; Berry, D.I.; Hirschi, J.J.-M. Drivers of exceptionally cold North Atlantic Ocean temperatures and their link to the 2015 European heat wave. *Environ. Res. Lett.* **2016**, *11*, 074004. [\[CrossRef\]](#)
18. Dong, B.; Sutton, R.; Shaffrey, L.; Wilcox, L. The 2015 European heat wave. *Spec. Suppl. Bull. Am. Meteorol. Soc.* **2016**, *97*, S14–S18. [\[CrossRef\]](#)
19. Meehl, G.A.; Tebaldi, C. More intense, more frequent, and longer lasting heat waves in the 21st century. *Science* **2004**, *305*, 994–997. [\[CrossRef\]](#) [\[PubMed\]](#)
20. Schär, C.; Vidale, P.L.; Lüthi, D.; Frei, C.; Häberli, C.; Liniger, M.; Appenzeller, C. The role of increasing temperature variability in European summer heat waves. *Nature* **2004**, *427*, 332–336. [\[CrossRef\]](#)
21. Jarzyna, K. Thermal stress diversity during heat waves in the Kielecka Upland in the beginning of XXI century. *Monit. Sr. Przyr.* **2012**, *13*, 41–50. (In Polish)
22. Kossowska-Cezak, U.; Skrzypczuk, J. Hot weather in Warsaw (1947–2010). *Prace Studia Geogr.* **2011**, *47*, 139–146. (In Polish)
23. Twardosz, R.; Kossowska-Cezak, U. Exceptionally hot summers in Central and Eastern Europe (1951–2010). *Theor. Appl. Clim.* **2013**, *112*, 617–628. [\[CrossRef\]](#)
24. Krzyżewska, A.; Wereski, S. Heat waves and frost waves in selected Polish stations against bioclimatic regions background (2000–2010). *Przegląd Geofiz.* **2011**, *56*, 99–109. (In Polish)
25. Porebska, M.; Zdunek, M. Analysis of extreme temperature events in Central Europe related to high pressure blocking situations in 2001–2011. *Meteorol. Z.* **2013**, *22*, 533–540. [\[CrossRef\]](#)
26. Tomczyk, A.M.; Bednorz, E. Heat waves in Central Europe and their circulation conditions. *Int. J. Climatol.* **2016**, *36*, 770–782. [\[CrossRef\]](#)
27. Wibig, J. Heat waves in Poland in the period 1951–2015: Trends, patterns and driving factors. *Meteorol. Hydrol. Water Manag.* **2018**, *6*, 37–45. [\[CrossRef\]](#)

28. Leckebusch, G.C.; Ulbrich, U. On the relationship between cyclones and extreme windstorms over Europe under climate change. *Glob. Planet. Chang.* **2004**, *44*, 181–193. [\[CrossRef\]](#)
29. Leckebusch, G.C.; Weimer, A.; Pinto, J.G.; Reyers, M.; Speth, P. Extreme wind storms over Europe in present and future climate: A cluster analysis approach. *Meteorol. Z.* **2008**, *17*, 67–82. [\[CrossRef\]](#)
30. Bielec-Bąkowska, Z. *Strong Anticyclones over Europe (1951–2010)*; Wydawnictwo Uniwersytetu Śląskiego: Katowice, Poland, 2014; p. 219. (In Polish)
31. Zhao, W.; Zhou, N.; Chen, S. The record-breaking high temperature over Europe in June of 2019. *Atmosphere* **2020**, *11*, 524. [\[CrossRef\]](#)
32. Deng, K.Q.; Yang, S.; Ting, M.F.; Lin, A.L.; Wang, Z.Q. An intensified mode of variability modulating the summer heat waves in Eastern Europe and Northern China. *Geophys. Res. Lett.* **2018**, *45*, 11361–11369. [\[CrossRef\]](#)
33. Trenberth, K.E.; Fasullo, J.T. Climate extremes and climate change: The Russian heat wave and other climate extremes of 2010. *J. Geophys. Res. Atmos.* **2012**, *117*, D17103. [\[CrossRef\]](#)
34. Fischer, E.M.; Seneviratne, S.I.; Luthi, D.; Schar, C. Contribution of land-atmosphere coupling to recent European summer heat waves. *Geophys. Res. Lett.* **2007**, *34*, L06707. [\[CrossRef\]](#)
35. Miralles, D.G.; Teuling, A.J.; van Heerwaarden, C.C.; de Arellano, J.V.G. Mega-heatwave temperatures due to combined soil desiccation and atmospheric heat accumulation. *Nat. Geosci.* **2014**, *7*, 345–349. [\[CrossRef\]](#)
36. Kalnay, E.; Kanamitsu, M.; Kistler, R.; Collins, W.; Deaven, D.; Gandin, L.; Iredell, M.; Saha, S.; White, G.; Woollen, J.; et al. The NCEP/NCAR 40-year reanalysis project. *Bull. Am. Meteorol. Soc.* **1996**, *77*, 437–471. [\[CrossRef\]](#)
37. Bartoszek, K.; Krzyżewska, A. The atmospheric circulation conditions of the occurrence of heatwaves in Lublin, southeast Poland. *Weather* **2017**, *72*, 176–180. [\[CrossRef\]](#)
38. Tomczyk, A.M.; Bednorz, E. Heat waves in Central Europe and tropospheric anomalies of temperature and geopotential heights. *Int. J. Climatol.* **2019**, *9*, 4189–4205. [\[CrossRef\]](#)
39. Owczarek, M.; Filipiak, J. Contemporary changes of thermal conditions in Poland, 1951–2015. *Bull. Geogr.* **2016**, *10*, 31–50. [\[CrossRef\]](#)
40. Frich, P.; Alexander, L.V.; Della-Marta, P.; Gleason, B.; Haylock, M.; Klein Tank, A.M.G.; Peterson, T. Observed coherent changes in climatic extremes during 2nd half of the 20th century. *Clim. Res.* **2002**, *19*, 193–212. [\[CrossRef\]](#)
41. Rey, G.; Jougl, E.; Fouillet, A.; Pavillon, G.; Bessemoulin, P.; Clavel, J.; Hémon, D. The impact of major heatwaves on all-cause and cause specific mortality in France 1971–2003. *Int. Arch. Occup. Environ. Health* **2007**, *80*, 615–626. [\[CrossRef\]](#) [\[PubMed\]](#)
42. Tomczyk, A.M.; Bednorz, E. Heat and cold waves on the southern coast of the Baltic Sea. *Baltica* **2014**, *27*, 45–53. [\[CrossRef\]](#)
43. Sulikowska, A.; Wypych, A.; Woszczek, I. Heatwaves in summer 2015 and their circular conditions. *Bad. Fizj.* **2016**, *A67*, 205–223. (In Polish)
44. Tomczyk, A.M.; Bednorz, E.; Pótrolniczak, M.; Kolendowicz, L. Strong heat and cold waves in Poland in relation with the large-scale atmospheric circulation. *Theor. Appl. Climatol.* **2019**, *37*, 1909–1923. [\[CrossRef\]](#)
45. Wibig, J. Waves of warm and coldness in Central Poland on the example of Łódź. *Acta Univ. Lodz. Folia Geogr. Phys.* **2007**, *8*, 27–61. (In Polish)
46. Wypych, A.; Sulikowska, A.; Ustrnul, Z.; Czekierda, D. Temporal Variability of Summer Temperature Extremes in Poland. *Atmosphere* **2017**, *8*, 51. [\[CrossRef\]](#)
47. Kejna, M.; Rudzki, M. Spatial diversity of air temperature changes in Poland in 1961–2018. *Theor. Appl. Climatol.* **2021**, in press. [\[CrossRef\]](#)
48. Tomczyk, A.M.; Owczarek, M. Occurrence of strong and very strong heat stress in Poland and its circulation conditions. *Theor. Appl. Climatol.* **2020**, *139*, 893–905. [\[CrossRef\]](#)